# Three-Dimensional Microwave Breast Imaging: A Bounded, Multi-frequency Inverse Scattering Solution on a Uniform Voxel Mesh

***Jacob D. Shea*[1], *Panagiotis Kosmas*[1,2], *Susan C. Hagness*[1], *Barry D. Van Veen*[1]**

[1]Department of Electrical and Computer Engineering, University of Wisconsin – Madison, 1415 Engineering Drive, Madison, WI 53706, USA, shea@cae.wisc.edu, hagness@engr.wisc.edu, vanveen@engr.wisc.edu

[2]Div. of Engineering, Kings College London, Strand, London, W2CR 2LS, UK, panagiotis.kosmas@kcl.ac.uk

## Abstract

Three-dimensional inverse scattering solutions for wideband microwave imaging of the breast are often limited by the computational complexity of the problem. We present a computationally tractable inverse scattering solution for a high-resolution discretization of the breast interior. Our technique is demonstrated by its application to an anatomically realistic numerical breast phantom, and the computational efficiency of the approach is detailed. We also show that unconstrained techniques of dielectric profile estimation are vulnerable to violation of physical bounds. A method of integrating bound constraints into the inversion algorithm is implemented and comparative results are presented.

## 1. Introduction

Inverse scattering methods are a significant focus of active research in the area of microwave medical imaging of the breast (see for example [1]). These methods seek to reconstruct the complete dielectric profile of the breast interior based on measurements of microwaves sourced and received by an array of antennas surrounding the breast. Due to the heterogeneity of the breast interior, the relationship between the dielectric profile and the scattering response is nonlinear. Iterative methods, such as the Distorted Born Iterative Method (DBIM) [2], are used to improve reconstruction of the heterogeneities that create the nonlinear scattering response.

Formulations of the inverse scattering problem for microwave breast imaging are varied and are often constrained by computational considerations. As a result, two-dimensional representations of the problem [3] are often pursued. Three-dimensional solutions are of great practical interest but can present a prohibitive computational burden. Similarly, wideband solutions can improve the resolution and stability of imaging algorithms over that of single frequency solutions at the expense of increased computational complexity. A solution on a fine uniform mesh in two dimensions (pixels) or three dimensions (voxels) uses a large number of unknowns that greatly exceeds the degrees of freedom of the system. However, simply decreasing the grid resolution would introduce unacceptable discretization error. It is therefore desirable to have a solution of sufficient resolution available for the exploration of the wideband three-dimensional imaging problem.

The inverse of the approximate linear system formed at each step of the DBIM has previously been solved using unconstrained techniques of optimization. However, permittivity and conductivity have physical lower bounds. Any nonphysical values in the estimated profile must then be corrected prior to computation of scattered fields. Typically, the nonphysical values are simply fixed at their respective bounds. Due to the interdependence of the solution elements, enforcing bounds in this manner on unconstrained solutions of the linear system can result in a suboptimal reconstruction when the extent of the bound violation is significant. We propose applying methods of bound-constrained optimization during the inversion of the linear system. In addition, both upper and lower bounds on the dielectric properties of breast tissue have been established recently [4] and are used to constrain the solution space even further.

In this paper, we image the breast in three dimensions on a high resolution grid using data from multiple microwave frequencies. In addition, we have integrated realistic bound constraints on the complex permittivity of breast tissues into the inverse solution. Section 2 summarizes the inverse scattering solution and describes both the inversion of the large-scale linear system and a method of imposing bound constraints during the inversion. These techniques are applied in Section 3 to a realistic numerical phantom derived from a magnetic resonance image (MRI), and comparative results are presented. Section 4 presents the computational tools employed in our imaging testbed and the time to solution for each step of the imaging process. Concluding remarks on the techniques and their results are offered in Section 5.

## 2. Solution Strategy

We use the DBIM to reconstruct the dielectric profile of the breast interior, as in [5-6]. At each iteration of our DBIM, the electric field scattered by the current estimate of the dielectric profile is computed using FDTD and is termed the forward solution. The heterogeneous Green's functions are also obtained from the FDTD computation. The residual error between the forward solution and the measured data is related to the error in the profile estimate by an electric field integral equation, which is made linear with respect to the unknown profile using the distorted Born approximation [2]. The integral equation is discretized to form a linear system which approximately maps the profile error to the scattering error. The inverse solution of the linear system is used to update the profile estimate and the algorithm iterates using the updated estimate. Given a reasonable initial estimate and careful approximation of the inverse solution, successive refinement of the profile by the DBIM leads to a stationary solution of the nonlinear scattering problem.

### 2.1 CGLS-Regularized Inverse Solution

The linear system of unknown grid parameters formed at each DBIM iteration is large-scale and highly underdetermined. In addition, the number of measurements is limited and the detail of the heterogeneity in the breast phantom is much finer than the resolution afforded by the illuminating wavelengths. Thus, the system is ill-posed and rank-deficient and requires regularization when approximating the inverse solution.

The computational requirements of many inverse techniques become prohibitively expensive for the large-scale system of a fine-grid discretization. Many regularization techniques require a series of trial solutions, such as the L-Curve Tikhonov method used in [5], but such methods are computationally impractical for the size of the system. We forego the determination of any preliminary regularization parameter and instead achieve regularization by early termination of the conjugate gradient for least squares (CGLS) algorithm applied to the normal equations. The self-regularizing behavior of conjugate gradient methods is discussed in [7], and has previously been employed in the context of the two-dimensional [8] and three-dimensional [6] breast imaging problems. We find a fixed number of iterations to be a sufficient stopping condition, although more sophisticated termination heuristics are available.

The matrix associated with the large-scale linear model is too large to be stored in memory. However, the CGLS algorithm does not use any matrix factorizations and requires only two matrix-vector multiplications per iteration [7]. Thus, the CGLS implementation need not have access to the entire matrix at any one time. The matrix-vector multiplications can be performed in pieces, with each row or sub-block of the matrix recomputed as needed.

### 2.2 Bound-Constrained Inverse Solution

The dielectric properties of breast tissue are physically bounded below by the properties of lipids and bounded above by the properties of saline. These frequency dependent properties may be even more tightly bounded using data from studies of breast tissues [4]. This data can be fit to single-pole Debye curves as in [9]. For a wideband problem expressed in the Debye parameter space, the frequency dependent upper and lower bounds on the dielectric properties are fit to the Debye model to create the respective upper and lower bounds for the Debye parameter unknowns.

We have observed that the extent of the bound violations in unconstrained solutions may worsen with increased tissue heterogeneity and may vary with the regularization technique. In addition, this condition does not disappear as the DBIM algorithm converges. Restricting the solution space of the underdetermined inverse problem will promote iterates with lower relative error and lead the DBIM to converge to a superior solution.

In order to evaluate the effect of bound violations on the quality of the solution, we implement a constrained inverse solution technique that is based on our existing method of approximating the inverse. We use the Projected-Restarted conjugate gradient method of enforcing nonnegativity constraints [10]. The method employs early termination regularization; the discrepancy principle and a fixed iteration limit are used as the stopping criteria for the CGLS algorithm. When a stopping condition is reached, the inversion algorithm iteratively restarts after projecting the solution onto the nonnegative set. It is straightforward to adapt the projection technique for non-zero lower and upper bounds. We use a slight variation of the Projected-Restarted CG method which better suits our need to conserve the total number of CG iterations.

## 3. Testbed and Results

We apply the techniques summarized in Section 2 to a heterogeneously dense breast phantom (ID#080304) selected from the UWCEM Numerical Breast Phantom Repository [9]. A homogeneous spherical inclusion with a 1-cm-diameter is positioned at a fibroglandular tissue site to represent a malignant tumor. All tissue types are modeled as single-pole Debye materials based on a dielectric property characterization of breast tissues [4]. Bistatic scattering measurements are simulated for a 40-element cylindrical array of dipoles using a three-dimensional Finite Difference Time Domain (FDTD) code on a uniform 0.5 mm grid of voxels. The reconstruction domain is discretized by a uniform 2.0 mm grid. The forward solution and heterogeneous Green's functions are computed by FDTD on the 2.0 mm grid, providing a minimum of ten samples per wavelength in the densest areas of the reconstructed profile. The observed time-domain fields are converted to phasor form at the frequencies of interest. The dielectric properties of the down-sampled skin region are assumed known, limiting the reconstruction region to the 69,496 voxels of the interior breast volume. The scattering integral equation is discretized at each interior voxel of the uniform 2.0 mm grid.

We employ a single-pole Debye model to capture the frequency dependent behavior of the unknown complex permittivity within each homogeneous voxel. The time constant of the single pole is assumed fixed and known, so that each voxel is represented by three unknowns: the static permittivity, the infinite permittivity, and the static conductivity. Phasor scattering data at six frequencies spanning 1.2-2.7 GHz are taken from each of the 780 unique bistatic transmission channels. The real and imaginary parts of the scattering equations are then separated so that the system is consistent with the real-valued Debye unknowns. The resulting linear system has 9,360 equations in 208,488 unknowns.

Cross-sections of the estimated permittivity and conductivity profiles after eight iterations of the DBIM are imaged at 1.5 GHz in Figure 1. Three pairs of images are displayed: the exact phantom profile and both the unbounded and bounded estimates of the profile. Areas of shallow bound violations can be seen in the unbounded estimate. The norm of the residual scattering error of the bounded estimate is 17% lower after eight iterations than that of the unbounded estimate. In addition, the constrained solution method increases the magnitude of the tumor in the difference between the tumor and tumor-free reconstructions. The improvement in the reconstruction of the inclusion is illustrated at 1.5 GHz by the color difference images of Figure 2.

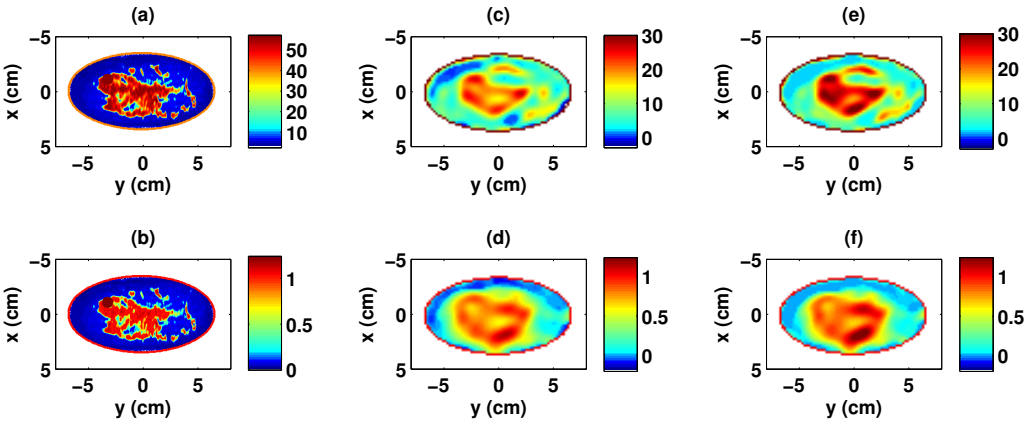


**Figure 1** – Cross-sectional color images of relative permittivity (top row) and effective conductivity in S/m (bottom row) at 1.5 GHz: (a)-(b) exact phantom profile, (c)-(d) unbounded estimate, (e)-(f) bounded estimate.

## 4. Computational Assessment

Three computational engines are used to complete the data acquisition and imaging process. Scattering data is simulated by FDTD using a multi-processor Fortran code running on a computing cluster. The forward solution at each step of the DBIM is computed by FDTD on the GPU of the Acceleware A20 hardware accelerator. The inverse solution is computed in a 32-bit version of Matlab running on a dual-core 2.0GHz processor and using up to 3.2GB of RAM in a 64-bit Windows environment. Single-precision values are used for all data and variables.

The acquisition of scattering data by FDTD at a 0.5 mm uniform grid resolution requires roughly 350 processor-hours and is distributed over several quad-core nodes on the computing cluster. The acquisition is

repeated to obtain calibration data with the antenna array in a homogeneous background medium. Each FDTD forward solution of 641,136 cells at a 2.0 mm uniform grid resolution takes 20 minutes. The computational expense of inverting the square system of 208,488 normal equations at each DBIM step is proportional to the number of conjugate gradient iterations; each costs approximately 3 minutes. For the results of this paper, the CGLS algorithm is terminated after a total of five iterations. The steep cost of each CG iteration owes to the memory limitations of the environment. The matrix associated with the inverse problem is too large to store in memory, and must be recomputed twice per iteration. The image pairs of Figure 1 (c-f) are estimates of the complex permittivity profile after eight DBIM iterations, requiring a total of 4.5 hours per reconstruction.

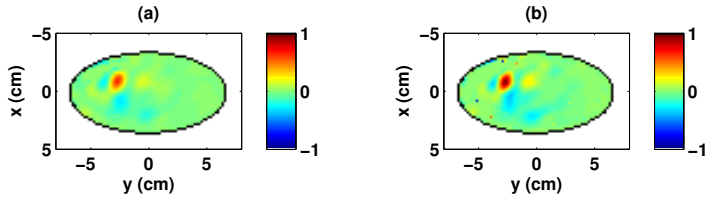


**Figure 2** – Difference of relative permittivity estimates with and without inclusion: (a) unbounded, (b) bounded.

## 5. Conclusion

We have demonstrated a wideband, three-dimensional inverse-scattering solution for breast imaging on a uniform 2.0 mm grid. The computational expense of the inverse solution is only incrementally greater than that of formulations of much smaller scale due to the efficiency of the CGLS regularization technique. For the purpose of achieving a tractable problem, the salient features of the early-termination CGLS approach are the inherent limitation of the number of CG iterations and the avoidance of any preliminary trial solutions. Implementation of a bounded solution was motivated by the observed violations of physical bounds by unconstrained formulations. The benefits of a constrained solution method are evidenced by the resulting decrease in solution error and the improvement in the reconstruction of a malignant inclusion.

## 6. References


1. P. M. Meaney, M. Fanning, D. Li, S. Poplack, and and K. D. Paulsen, "A clinical prototype for active microwave imaging of the breast," *IEEE Trans. Microwave Theory Tech.*, vol. 48, no. 11, pp. 1841-1853, Nov. 2000.

2. W. C. Chew, *"Waves and fields in inhomogeneous media,"* New York: Van Nostrand Reinhold, 1990.

3. P. M. Meaney, M. W. Fanning, T. Raynolds, C. J. Fox, Q. Q. Fang, C. A. Kogel, S. P. Poplack, and K. D. Paulsen, "Initial clinical experience with microwave breast imaging in women with normal mammography," *Academic Radiology*, vol. 14, no. 2, pp. 207–218, Feb 2007.

4. M. Lazebnik, L. McCartney, D. Popovic, C. B. Watkins, M. J. Lindstrom, J. Harter, S. Sewall, A. Magliocco, J. H. Booske, M. Okoniewski, and S. C. Hagness, "A large-scale study of the ultrawideband microwave dielectric properties of normal breast tissue obtained from reduction surgeries," *Phys. Med. Biol.*, vol. 52, pp.2637-2656, 2007.

5. D. Winters, *Dimensionality reduction in inverse scattering: Applications to microwave imaging for breast cancer detection*, PhD Thesis, University of Wisconsin-Madison, 2007

6. P. Kosmas, J. D. Shea, B. D. Van Veen, and S. C. Hagness, "Microwave imaging of realistic breast phantoms via a three-dimensional inexact Gauss-Newton algorithm," submitted to IEEE International Symposium on Antennas and Propagation, San Diego, CA, 2008.

7. P. C. Hansen, *Rank-Deficient and Discrete Ill-Posed Problems: Numerical Aspects of Linear Inversion,* Philadelphia: SIAM, 1998.

8. T. Rubæk, P.M.Meaney, P.Meincke, and K. D. Paulsen, "Nonlinear microwave imaging for breast-cancer screening using Gauss-Newton's method and the CGLS inversion algorithm," *IEEE Trans. Antennas Propag.*, vol. 55, no. 8, pp. 2320-2331, Aug. 2007.

9. E. Zastrow, S. K. Davis, M. Lazebnik, F. Kelcz, B. D. Van Veen, and S. C. Hagness, "Development of anatomically realistic numerical breast phantoms with accurate dielectric properties for modeling microwave interactions with the human breast", *IEEE Trans. Biomed. Eng.*, submitted. [Database available online: http://uwcem.ece.wisc.edu/]

10. D. Calvetti, G. Landi, L. Reichel, and F. Sgallari, "Non-negativity and iterative methods for ill-posed problems," *Inv. Prob.*, vol. 20, pp. 1747-1758, 2004.